Performance Analysis of SIR-Based Dual Selection Diversity Over Correlated Nakagami-m Fading Channels

George K. Karagiannidis, *Member, IEEE*

***Abstract*—Signal-to-interference-ratio (SIR)-based selection diversity is an efficient technique to mitigate fading and cochannel interference in wireless communications systems. In this paper, an approach to the performance analysis of dual SIR-based selection diversity over correlated Nakagami-m fading channels with arbitrary parameters is presented. Useful formulae for the outage probability, the average output SIR, and the average error probability for coherent, noncoherent, and multilevel modulation schemes are derived. The main contribution of this paper is that, for the first time, the proposed analysis is carried out assuming correlated Nakagami-m fading with arbitrary parameters for both the desired signals and the cochannel interferers, which is the real scenario in practical dual selection diversity systems with insufficient antenna spacing. It is shown that the general results presented in the paper reduce to the specific ones for the independent fading case, previously published. Numerical and simulation results are also presented to show the effects of various parameters as the fading severity, input SIR unbalance, and level of correlation to the system's performance.**

***Index Terms*—Cochannel interference, correlated fading, diversity systems, Nakagami-m fading, Rayleigh fading, selection combining.**

I. INTRODUCTION

SEVERAL techniques have been proposed to mitigate the effects of fading and cochannel interference, in order to increase the system's capacity and to improve the offered quality-of-service (QoS) in wireless communications systems. Such techniques are diversity reception, dynamic channel allocation, and power control. Among them, diversity reception using multiple antennas at the receiver (space diversity) has long been recognized as a very effective method to improve the system's QoS [1]. The most popular space-diversity techniques are selection combining (SC), equal-gain combining (EGC), maximal-ratio combining (MRC), or a combination of MRC and SC called generalized selection combining (GSC) [1], [2]. Among these diversity schemes, SC is the least complicated, since the processing is performed only on one of the diversity branches and no channel information is required. Traditionally, in SC the combiner chooses the branch with the highest signal-to-noise ratio (SNR), which corresponds to the strongest signal if equal noise power is assumed among the branches [2]. Other researchers have proposed the selection of the branch with the highest signal-plus-noise (SPN) [3]. However, in interference-limited fading environments as in cellular communications systems where the level of the cochannel interference is sufficiently high as compared to the thermal noise, the most effective performance criterion is to select the highest signal-to-interference ratio (SIR; SIR-based selection diversity) [4]. SIR can be measured in real time both in base stations (uplink) and in mobile stations (downlink) using specific SIR estimators as well as those for both analog [5]–[7] and digital wireless systems (e.g., GSM, IS-54) [8], [9].

In order to study the effectiveness of any modulation scheme and the type of diversity used, it is required to evaluate the system's performance over the channel conditions. Well-known measures, commonly used in wireless communications systems, are the outage probability, the average output SIR or SNR, and the average probability of bit error. In the literature, the performance analysis of diversity systems in the presence of cochannel interference has been studied extensively for several diversity schemes and by several researchers [10]–[19]. Most assume independent fading between the diversity branches and/or between the cochannel interferers. However, independent fading assumes antenna elements to be placed sufficiently apart, which is not always realized in practice due to insufficient antenna spacing when diversity is applied in small terminals. In such terminals equipped with multiple antennas, correlation arises between the diversity branches. A method for the evaluation of the outage probability in dual SIR-based SC with correlated fading, for both desired signals and interferers, has been published in [4], where a formulation for the outage probability was presented and, as mentioned above, the advantage of SIR-based over desired power-based selection combining was confirmed. However, this analysis is limited to the Rayleigh modeling for the cochannel interferers. Moreover, to the best of the author's knowledge, no analytical study investigating the average output SIR or the average probability of bit error of a dual SC receiver operating in correlative fading has been reported in the literature.

In this paper, an approach to the performance analysis of dual SIR-based SC over correlated Nakagami-m fading channels with arbitrary parameters is presented. Useful formulae for the outage probability, average output SIR, and average error probability in noncoherent [binary differentially phase-shift keying (BDPSK) and binary frequency-shift keying (BFSK)], coherent [binary phase-shift keying (BPSK), orthogonal BFSK], quaternary differential phase-shift keying (DQPSK)

Manuscript received September, 6, 2002; revised February 25, 2003 and May 8, 2003.

The author is with the Institute for Space Applications and Remote Sensing, National Observatory of Athens, Athens 15236, Greece (e-mail: gkarag@space.noa.gr).

Digital Object Identifier 10.1109/TVT.2003.816612

with Gray coding and multilevel signaling [multiple phase-shift keying (MPSK) and multiple differential phase-shift keying (MDPSK)] are derived. The main contribution of this paper is that the proposed analysis is carried out assuming, for the first time, correlative Nakagami-m fading with arbitrary parameters for both the desired signals and the co-channel interferers, which is the real scenario in practical dual SC systems with insufficient antenna spacing. Numerical and simulation results are also presented to show the effects of various system's parameters, such as the fading severity, input SIR unbalance, and level of correlation to the system's performance.

The remainder of this paper is organized as follows. In Section II, the channel and system model are presented and the probability distribution function (pdf) and cumulative distribution function (cdf) of the SC output SIR are extracted in useful forms. In Section III, a formula for the outage probability is presented in the form of a convergent double sum. In Section IV, a useful formulation for the average output SIR is extracted in the form of a triple sum. Finally, in Section V, useful expressions are derived for the average error probability in several modulation schemes, since some concluding remarks are offered in Section VI. Sections II–V also include numerical results, simulations, and discussions to illustrate the proposed mathematical analysis.

II. Statistics of the SC Output SIR

A. Channel and System Model

In the last years, there has been a continuing interest in modeling various propagation channels with the Nakagami-m model, which describes multipath scattering with relatively large delay-time spreads, with different clusters of reflected waves [20]. It provides good fits to collected data in indoor and outdoor mobile-radio environments and is used in many wireless communications applications [21], [22]. In this paper, a wireless communication system with dual SIR-based SC diversity is considered. The desired signal received by the ith antenna, $D_i(t)$, can be written as [19]

$$D_i(t) = R_i(t)e^{j\phi_i(t)}e^{j[2\pi f_c t+\Phi(t)]}, \qquad i=1,2 \tag{1}$$

with f_c being the carrier frequency, $\Phi(t)$ the desired information signal, $R_i(t)$ a Nakagami-m distributed random amplitude process, and $\phi_i(t)$ the random phase uniformly distributed in $[0,2\pi]$. The resultant interfering signal received by the ith antenna is

$$C_i(t) = r_i(t)e^{j\theta_i(t)}e^{j[2\pi f_c t+\psi(t)]}, \qquad i=1,2 \tag{2}$$

where $r_i(t)$ is also a Nakagami-m distributed random amplitude process, $\theta_i(t)$ is the random phase, and $\psi(t)$ is the information signal. This model refers to the case of a single cochannel interferer. However, the general case of multiple interferers can be also approximately modeled with (1) and (2), taking into account that the sum of K independent identically distributed (i..i.d.) Nakagami-m random variables (RV) can be accurately approximated by another Nakagami-m distribution with a parameter ${}_0m$ and mean power ${}_0\Omega$ given by [20, p. 22]

$$\begin{aligned} {}_om &= mK \\ {}_o\Omega &= K\Omega\left(1+(K-1)\frac{\Gamma^2\left(m+\frac{1}{2}\right)}{m\Gamma^2(m)}\right) \\ &\cong K^2\Omega\left(1-\frac{1}{5m}\right). \end{aligned} \tag{3}$$

The case of i.i.d. interferers is not unreasonable in practical applications, since interferers originated from approximately the same distance from the receiver can be assumed to have the same average powers. Moreover, the performance of the SC can be carried out by considering, as Winters in [18], the effect of only the strongest interferer, assuming that the remaining interferers are combined and considered as lumped interference that is uncorrelated between antennas. Furthermore, $R_i(t)$, $r_i(t)$, $\phi_i(t)$, and $\theta_i(t)$are assumed to be mutually independent and the level of the interference is sufficiently high for the effect of thermal noise on system performance to be negligible (interference-limited environment) [13]. Now, due to insufficient antennae spacing, both desired and interfering signal envelopes experience correlative Nakagami-m fading with joint pdfs [20]

$$\begin{aligned} f_{R_1,R_2}(R_1,R_2) =& \frac{4m_d^{m_d+1}(R_1R_2)^{m_d}}{\Gamma(m_d)\Omega_{d1}\Omega_{d2}(1-\rho)\left(\sqrt{\rho\Omega_{d1}\Omega_{d2}}\right)^{m_d-1}} \\ &\times e^{-(m_dR_1^2+R_2^2/\sqrt{\Omega_{d1}\Omega_{d2}(1-\rho)}} \\ &I_{m_d-1}\left(\frac{2\sqrt{\rho}m_dR_1R_2}{\sqrt{\Omega_{d1}\Omega_{d2}}(1-\rho)}\right) \end{aligned} \tag{4}$$

and

$$\begin{aligned} f_{r_1,r_2}(r_1,r_2) =& \frac{4m_c^{m_c+1}(r_1r_2)^{m_c}}{\Gamma(m_c)\Omega_{c1}\Omega_{c2}(1-\rho)\left(\sqrt{\rho\Omega_{c1}\Omega_{c2}}\right)^{m_c-1}} \\ &e^{-(m_cr_1^2+r_2^2)/\sqrt{\Omega_{c1}\Omega_{c2}(1-\rho)}} \\ &I_{m_c-1}\left(\frac{2\sqrt{\rho}m_cr_1r_2}{\sqrt{\Omega_{c1}\Omega_{c2}}(1-\rho)}\right) \end{aligned} \tag{5}$$

whereas $\Gamma(\cdot)$ is the Gamma function, $I_v(\cdot)$ being the first kind and νth order modified Bessel function, ρ the correlation coefficient, $\Omega_{di}=\overline{R_i^2}$ and $\Omega_{ci}=\overline{r_i^2}$ the average signal desired and interference powers at the ith branch, and m_d, m_c the fading severity parameters for the desired and interference signal, correspondingly. Let $\zeta_1=R_1^2/r_1^2$ and $\zeta_2=R_2^2/r_2^2$ be the instantaneous SIRs at the input diversity branches. The selection combiner chooses and outputs the branch with the largest SIR[1]

$$\zeta=\zeta_{\mathrm{OUT}}=\max\left(\zeta_1,\zeta_2\right). \tag{6}$$

[1]The proposed in this paper analysis can be modified to include the effect of thermal noise on system performance, when it cannot be ignored. In this case, the selection is based on the signal-to-interference-plus-noise ratio (SINR), instead of SIR. The combiner chooses the branch with the largest instantaneous SINR between $\zeta_1=R_1^2/(r_1^2+\sigma^2)$ and $\zeta_1=R_1^2/(r_1^2+\sigma^2)$, with σ^2 being the noise power, equal for the two diversity paths.

TABLE I
TERMS NEED TO BE SUMMED IN (7) TO ACHIEVE ACCURACY AT THE SIGNIFICANT DIGIT PRESENTED IN THE BRACKETS

	m_d=3.2, m_c=1.3, S_1=S_2			
S_1/t \ ρ	-5 dB (6[th])	0 dB (6[th])	10 dB (7[th])	15 dB (9[th])
0.2	9	9	9	11
0.4	14	14	13	14
0.6	32	31	24	31
0.8	52	48	45	46

B. PDF and CDF of the SC Output SIR

If $S_1 = \Omega_{d1}/\Omega_{c1}$, $S_2 = \Omega_{d2}/\Omega_{c2}$ are the average SIRs at the two input branches of the SC, then the dual SIR-based SC output cdf can be expressed as (see Appendix I)

$$F_\zeta(t) = \sum_{i_1,i_2=0}^{\infty} \frac{G_1 t^{2(m_d+i_1)}}{\left(m_d t + m_c\sqrt{S_1S_2}\right)^{2(m_d+i_1)}} \times \left[{}_2F_1\left(i_1+m_d, 1-i_2-m_c; i_1+m_d+1; \frac{m_d t}{m_d t + m_c\sqrt{S_1S_2}}\right)\right]^2 \quad (7)$$

with

$$G_1 = \frac{m_d^{2(m_d+i_i)}(1-\rho)^{m_d+m_c}\rho^{i_1+i_2}[\Gamma(i_1+i_2+m_d+m_c)]^2}{\Gamma(m_d)\Gamma(m_c)i_1!i_2!\Gamma(m_d+i_1)\Gamma(m_c+i_2)(i_1+m_d)^2}$$

and ${}_2F_1(u_1,u_2;u_3;x)$ being the Gaussian hypergeometric function [23, (9.100)]. The nested double infinite sum in (7) converges for any value of the parameters ρ, m_c, m_d, S_1, and S_2. In Table I, the terms need to be summed to achieve a desired accuracy are depicted. As is shown in this table, the values of these terms are strongly related to the correlation coefficient ρ and increase as the correlation increases. For the special case of $m_d = 1$, $m_c = 1$ (Rayleigh-desired signal and cochannel interference), (7) gives the same results with [4, eq. (6)]. The pdf of the SC output SIR can be found using Appendix II and is depicted in (8) at the bottom of the page.

In Fig. 1, the pdf of the SC output SIR is plotted for balanced and unbalanced SIRs at the input branches. In this figure, the densities obtained by both the theory, using (8), and simulations are compared. Simulations were performed using the C^{++} programming language with the use of an algorithm included in [24]. For the generation of the correlated Nakagami-m envelopes, over a million samples were used. A very good match between the theory and simulations is evident from Fig. 1.

III. Outage Probability

Outage probability is a measure of the system's performance, used to control the cochannel interference level, helping the designers of wireless communications systems to readjust the system's operating parameters in order to meet the QoS and grade-of-service (GoS) demands. The term outage is related to the criterion used for the assessment of the satisfactory reception. In an interference-limited environment, the outage probability is defined as the probability of failing to achieve an SIR sufficient to give a radio reception over a level QoS, which is determined by a protection ratio [11], [25], [26]. If β is the protection ratio, defined as the ratio of the desired signal power to the interference power at the output of the combiner, the outage probability can be expressed as

$$P_{\mathrm{OUT}} = \text{Probability}\ (\zeta < \beta) = \int_0^\beta f_{\mathrm{SIR}}(t)dt = F_{\mathrm{SIR}}(\beta). \quad (9)$$

The protection ratio β depends upon the used modulation technique as well as on the desired QoS. Note that in the case of independent branches ($\rho = 0$), only the term $i_1 = 0$, $i_2 = 0$ of the summation over i_1, i_2 in (7) is nonzero. In this case, (7) is simplified to

$$P_{\mathrm{OUT}}|_{\rho=0} = \left[{}_2F_1\left(m_d, 1-m_c; m_d+1; \frac{m_d\beta}{m_d\beta + m_c\sqrt{S_1S_2}}\right) \times \frac{\beta^{m_d} m_d^{m_d-1}\Gamma(m_d+m_c)}{\Gamma(m_d)\Gamma(m_c)(m_d\beta + m_c\sqrt{S_1S_2})^{m_d}}\right]^2. \quad (10)$$

Also using [27, eq. (26.5.23)], [27, eq. (26.5.24)], and [27, eq. (6.2.2)] for $S_1 = S_2 = S$ and for integer $m_d = m_c = m$, (10) is reduced to a useful previous published result by Abu-Dayya and Beaulieu [19, eq. (37)].

In Fig. 2, the outage probability is plotted versus S_1, normalized by the protection ratio β for several values of m_d and m_c and for a fixed correlation coefficient ρ. Balanced $(S_1 = S_2)$ and unbalanced $(S_2 = S_1/4)$ SIRs are assumed at the two input branches. For $m_d = 1$ and $m_c = 1$ (Rayleigh-desired and cochannel interference), the results are similar with those corresponding in [4]. It is very interesting to observe here that for low values of S_1/β (<2 dB), the outage performance deteriorates when the fading severity of the interferers decreases (m_c increases), due to the superiority of the interference to the desired signal. But, for higher values of S_1/β (dominance of the desired signal), the fading severity of the interferers acts

$$f_\zeta(t) = 2\sum_{i_1,i_2=0}^{\infty} \frac{G_1(i_1+m_d)t^{2i_1+2m_d-1}m_c^{i_2+m_c}(S_1S_2)^{(i_2+m_c)/2}}{(m_d t + m_c\sqrt{S_1S_2})^{2(i_1+m_d)+i_2+m_c}} \times {}_2F_1\left(i_1+m_d, 1-i_2-m_c, i_1+m_d+1; \frac{m_d t}{m_d t + m_c\sqrt{S_1S_2}}\right). \quad (8)$$

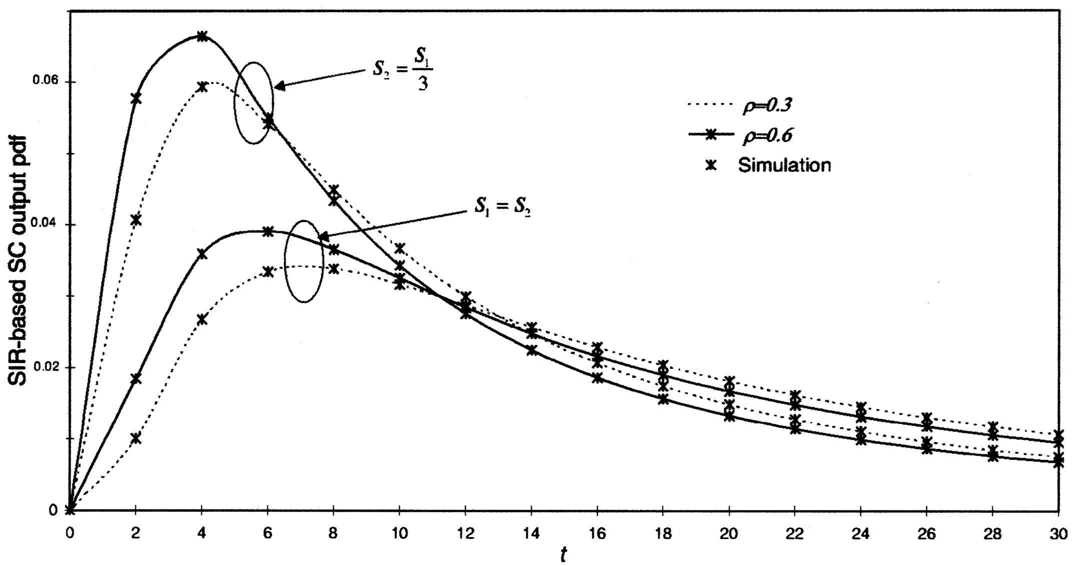

Fig. 1. SIR-based dual SC output pdfs ($m_c = 1.3$, $m_d = 3.1$).

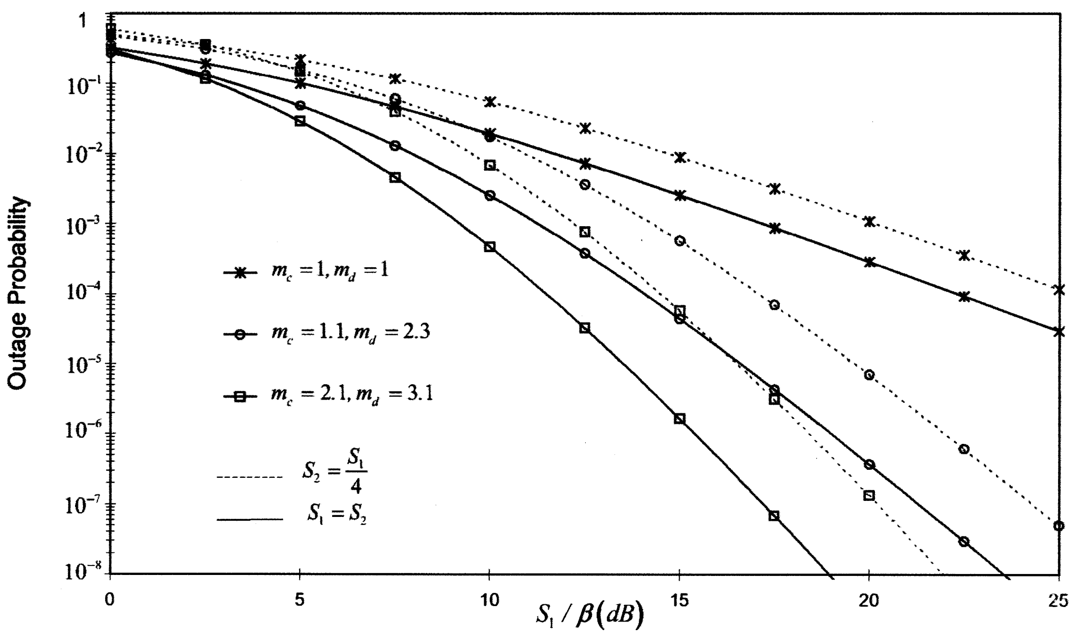

Fig. 2. Outage probability versus the S_1 normalized by the protection ratio β for $\rho = 0.5$.

inversely, leading to a decrease of the outage probability. In Fig. 3, the outage probability is plotted versus the correlation coefficient ρ, for several values of S_1/β, m_d, and m_c. Balanced $(S_1 = S_2)$; and unbalanced $(S_2 = S_1/4)$ SIRs. It is evident that, for $S_1/\beta = 0$ dB (strong interference) the outage probability increases slowly as the correlation coefficient increases, while a small increase in m_d does not have a significant effect on P_{out}. For higher values of S_1/β, as in the case of $S_1/\beta = 10$ dB, the influence of m_d and ρ on P_{out} becomes stronger.

IV. Average- Output SIR

Average-output SIR is another important performance criterion for SIR-based wireless communications systems operating in a cocannel interference environment. The average SIR $\bar{S}$ at the output of SC can be derived by averaging the instantaneous output SIR t over the pdf of t[2]. Hence, taking into account (8), $\bar{S}$ can be written as

$$\begin{aligned}\overline{S} =& \int_0^\infty t f_\zeta(t) dt \\ =& 2 \sum_{i_1,i_2=0}^{\infty} \frac{G_1(i_1+m_d)}{(S_1S_2)^{m_d+i_1}} \\ & \times \int_0^\infty t^{2i_1+2m_d} \\ & \times \left(1+\frac{m_d}{m_c}\frac{t}{\sqrt{S_1S_2}}\right)^{-2(i_1+m_d)-i_2-m_c} \\ & \times {}_2F_1\Bigg(i_1+m_d, 1-i_2-m_c, i_1 \\ & \qquad + m_d + 1; \frac{\frac{m_d}{m_c}\frac{t}{\sqrt{S_1S_2}}}{\frac{m_d}{m_c}\frac{t}{\sqrt{S_1S_2}}+1}\Bigg) dt. \quad (11)\end{aligned}$$

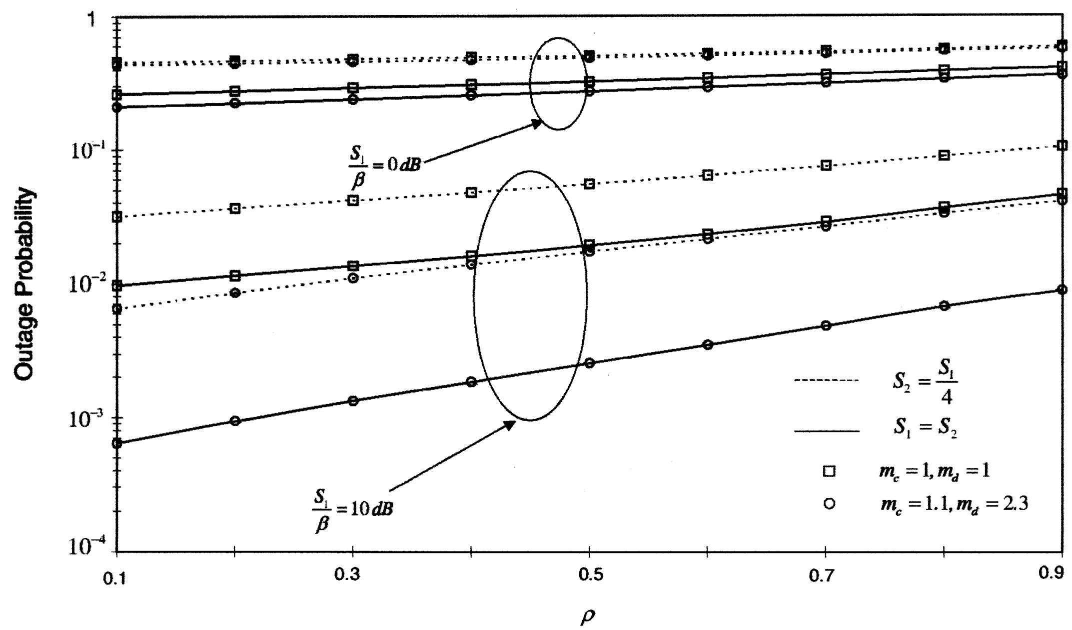

Fig. 3. Outage probability versus the correlation coefficient ρ.

Using the hypergeometric series form of ${}_2F_1(a,b,c,z) = \sum_{n=0}^{\infty}((a)_n(b)_n z^n/(c)_n n!)$[23, (9.100)] with $(\bullet)_n$ the Pochhammer symbols, defined as $(a)_n = \Gamma(a+n)/\Gamma(a)$, (11) can be written after some manipulations as

$$\overline{S} = 2\sum_{i_1,i_2,n=0}^{\infty} \frac{G_2}{(S_1S_2)^{m_d+i_1}}\left(\frac{m_d}{m_c}\frac{1}{\sqrt{S_1S_2}}\right)^n \times \int_0^{\infty} \frac{t^{2i_1+2m_d+n+1+-1}}{\left(1+\frac{m_d}{m_c}\frac{t}{\sqrt{S_1S_2}}\right)^{2(i_1+m_d)+i_2+m_c+n}}dt \quad (12)$$

with

$$G_2 = \frac{G_1(i_1+m_d)(i_1+m_d)_n(1-i_2-m_c)_n}{(i_1+m_d+1)_n n!}.$$

The integral in (12) has the form $\int_0^{\infty} x^{\mu-1}/(1+\lambda x)^v dx$ and can be solved using [23, (3.194/3)]. Hence, (12) can be finally expressed as

$$\overline{S} = 2\sqrt{S_1S_2} \sum_{i_1\cdot i_2\cdot n=0}^{\infty} G_3 B(2i_1+2m_d+n+1, i_2+m_c-1) \quad (13)$$

with $G_3 = G_2(m_d/m_c)^{-(2i_1+2m_d+1)}$ and $B(x,y)$ is the Beta function [23, (8.38)]. It must be noted here that, due to the form of G_2 and the Beta function in (13), m_c should not take integer values. But this is not a serious trouble in our analysis, since in practical applications, m_c never takes integer values. For $\rho = 0$, (13) is simplified to

$$\overline{S}|_{\rho=0} = 2\sqrt{S_1S_2}\sum_{n=0}^{\infty}\left[\frac{\Gamma(m_d+m_c)}{\Gamma(m_d)\Gamma(m_c)}\right]^2 \times \frac{(1-m_c)_n m_c^{2m_d+1}}{m_d\Gamma(m_d+n+1)} \times B(2m_d+n+1, m_c-1). \quad (14)$$

Into the following, numerical results are presented to illustrate the formulation presented above. More specifically, the effect of the cochannel interference and the fading correlation to the output average SIR is investigated. In Fig. 4, the first branch-normalized output SIR versus the correlation coefficient ρ is depicted for equal $(S_1 = S_2)$ and unequal $(S_2 = S_1/4)$ branch input mean SIRs and for several values of the fading severities m_d and m_c. It is observed here that, with m_c constant, the effect of m_d to the diversity gain performance is small. Moreover, diversity gain decreases with an increase of the correlation, as expected. Finally, the output-average SIR decreases as the parameter m_d increases. Similar behavior is also observed in [28], where the average output SNR of a dual SC was studied. It is interesting to note here that diversity gain changes rapidly with a small change of m_c. This is evident in Fig. 5, where the first branch-normalized output SIR versus the cochannel fading severity parameter m_c is depicted. A significant improvement at the diversity gain is observed for lower values of $m_c (m_c < 2)$. From the mathematical point of view, this behavior is due to the widespread of the output SIR pdf, (37), for small values of m_c. From the physical point of view, lower values of m_c mean deep fading behavior for the cochannel interferers that lead to an increase of the average SIR at the output of the SC. The fading severity of the interference plays the main role to output SIR performance. It must be noted here that for $m_c = 1$, the computed values of $\bar{S}/S_1$ are exactly the same with the corresponding ones produced after processing of the formulae presented in [4].

V. Average Error Probability

The average error probability at the output of the SC $\bar{P}_e$ can be derived by averaging the conditional error probability $P_e(t)$ over the pdf of the SC output SIR, i.e.,

$$\overline{P}_e = \int_0^{\infty} f_{\zeta}(t)P_e dt. \quad (15)$$

A. Noncoherent Binary Signaling

For BDPSK and non-coherent BFSK P_e is given by [1]

$$P_e(t) = \frac{1}{2}e^{-gt}. \quad (16)$$

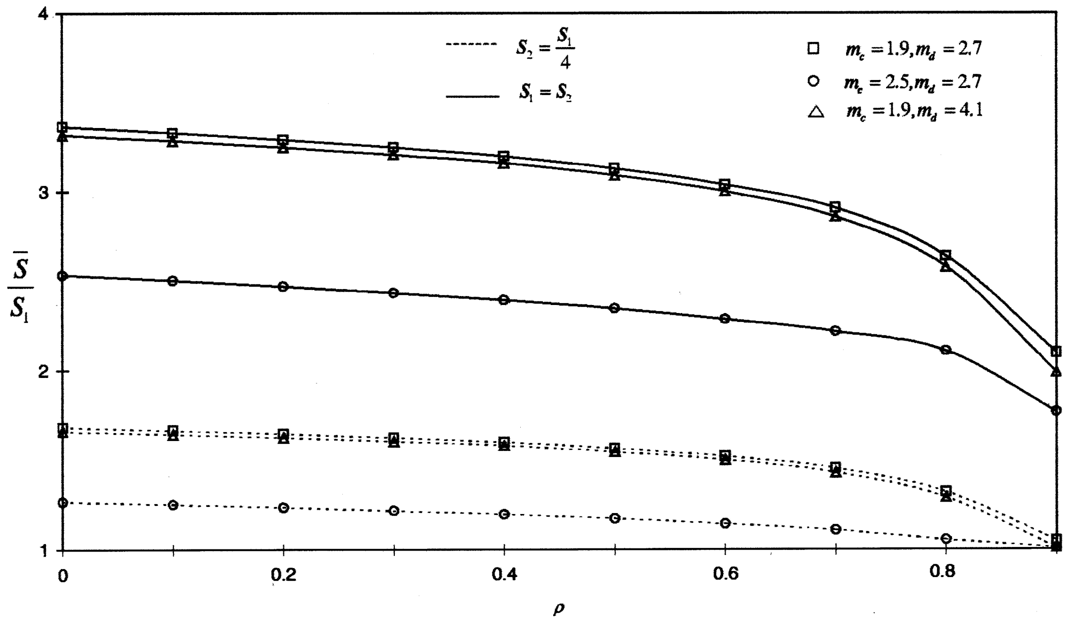

Fig. 4. First branch-normalized output SIR versus the corelation coefficient ρ.

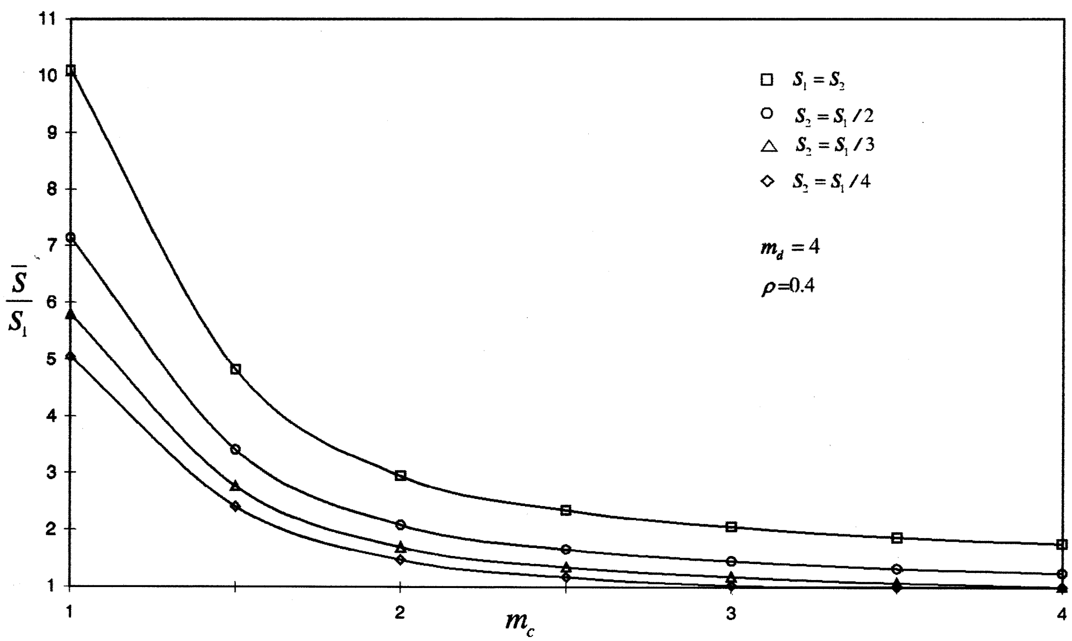

Fig. 5. First branch-normalized output SIR versus the cochannel fading parameter m_c.

Using (15) and (16) and following the same procedure as in Section IV, $\overline{P_e}$ can be written as

$$\overline{P}_e = \sum_{i_1,i_2,n=0}^{\infty} \frac{G_2}{(S_1S_2)^{m_d+i_1}} \left(\frac{m_d}{m_c}\frac{1}{\sqrt{S_1S_2}}\right)^n \times \int_0^\infty e^{-gt} t^{(2i_1+2m_d+n)-1} \left(1+\frac{m_d t}{m_c\sqrt{S_1S_2}}\right)^{-[2(i_1+m_d)+i_2+m_c+n]dt}. \quad (17)$$

The integral in (17) has the form $\int_0^\infty e^{-gx}x^{\mu-1}(1+\lambda x)^{-v}dx$ and can be solved using [23, (3.383/5)], resulting finally in

$$\overline{P}_e = \sum_{i_1,i_2,n=0}^{\infty} \left(\frac{m_d}{m_c}\right)^{-(2_i+2m_d)} \times G_2\sqrt{S_1S_2}\Gamma(2i_1+2m_d+n) \times \Psi\left(2i_1+2m_d+n, 1-i_2-m_c; \frac{g}{\frac{m_d}{m_c\sqrt{S_1S_2}}}\right) \quad (18)$$

with $\Psi(a,b;z)$ being a type of the confluent hypergeometric function defined in [23, eqs. (9.210/2), (9.211/4)]. For $\rho = 0$, (18) is simplified to

$$\bar{P}_e|_{\rho=0} = \sqrt{S_1S_2}\sum_{n=0}^{\infty}\left[\frac{\Gamma(m_d+m_c)}{\Gamma(m_d)\Gamma(m_c)}\right]^2 \frac{\Gamma(2m_d+n)}{(m_d+n)\Gamma(1+n)} \times (1-m_c)_n m_c^{2m_d}\Psi\left(2m_d+n, 1-m_c; \frac{g}{\frac{m_d}{m_c\sqrt{S_1S_2}}}\right). \quad (19)$$

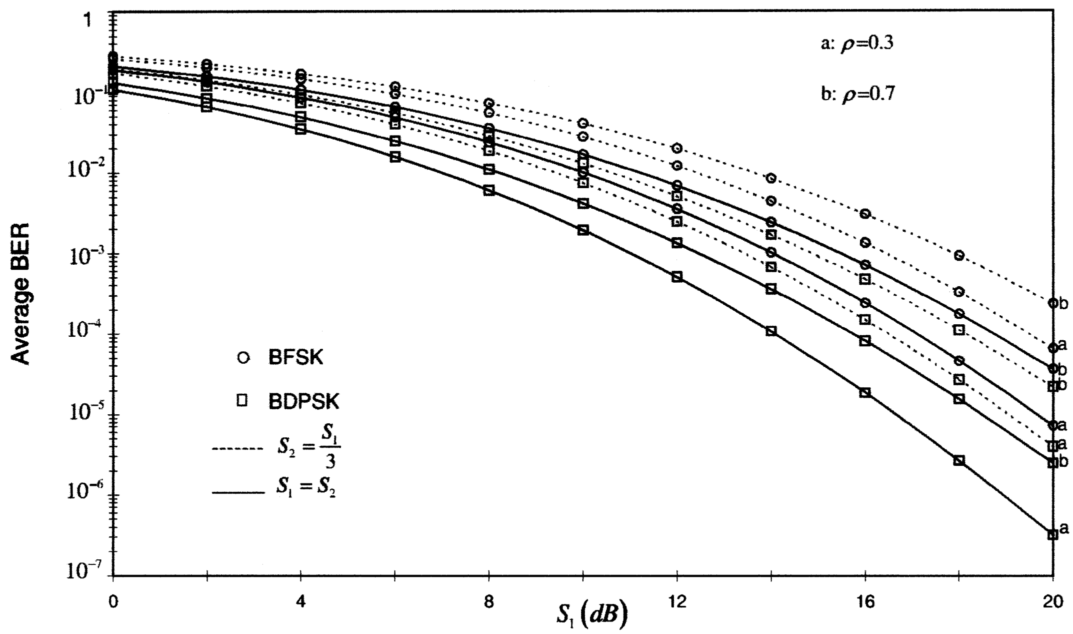

Fig. 6. Average BER versus S_1 in noncoherent BDPSK and BFSK for $m_c = 1.5$, $m_d = 2.9$.

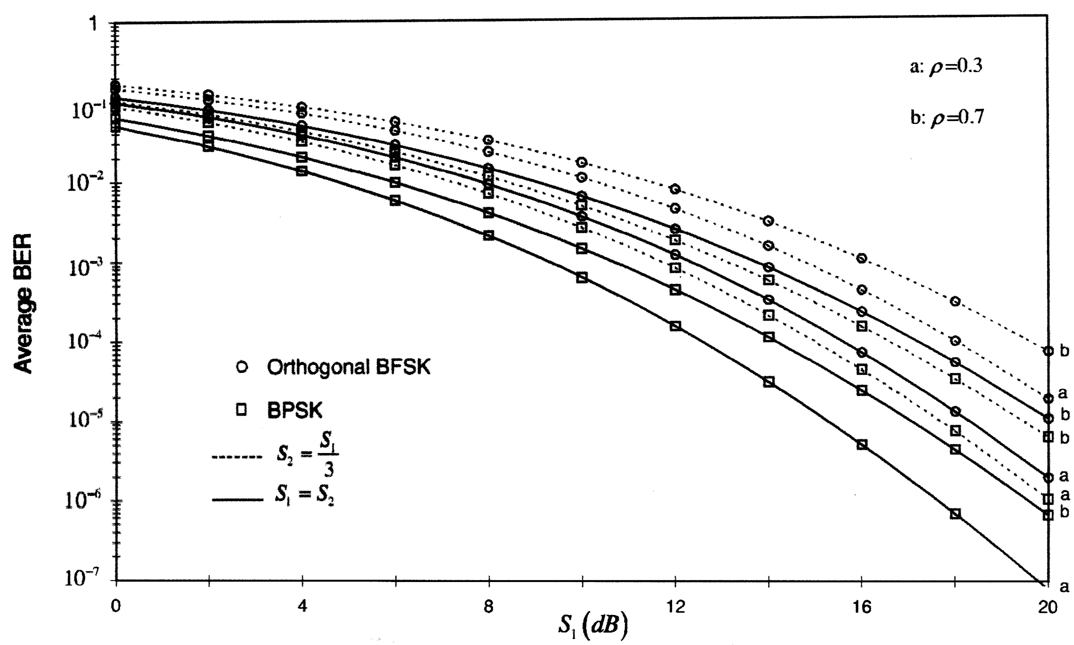

Fig. 7. Average BER versus S_1 in coherent BPSK and orthogonal BFSK for $m_c = 1.5$, $m_d = 2.9$.

In Fig. 6, $\bar{P}_e$ is plotted versus the S_1, for $m_d = 2.9$, $m_c = 1.5$ and several values for the correlation coefficient ρ, assuming BDPSK modulation. Balanced $(S_1 = S_2)$ and unbalanced $(S_2 = S_1/3)$ SIRs are assumed at the two input branches. In the same figure, $\bar{P}_e$ is depicted for noncoherent BFSK, assuming the same values for the system's parameters as in BDPSK.

B. Coherent Binary Signaling

In the case of BPSK and orthogonal BFSK, the conditional error probability can be written using an alternate representation of the Gaussian Q-function as [29], [30]

$$P_e(t) = \frac{1}{\pi}\int_0^{\pi/2} e^{-g/\sin^2\theta t} d\theta. \tag{20}$$

Now, working as in [29], it can be easily recognized that there is a similarity between (16) and (20), which allows us to write $\bar{P}_e$ directly as

$$\begin{aligned}\bar{P}_e =& \frac{1}{\pi}\sum_{i_1,i_2,n=0}^{\infty}\left(\frac{m_d}{m_c}\right)^{-(2i_1+2m_d)} \\ &\times G_2\sqrt{S_1S_2}\Gamma(2i_1+2m_d+n) \\ &\times \int_0^{\pi/2}\Psi\left(2i_1+2m_d+n, 1-i_2-m_c; \frac{g(\theta)}{\frac{m_d}{m_c}\frac{1}{\sqrt{S_1S_2}}}\right) \\ &\times d\theta \end{aligned} \tag{21}$$

with $g(\theta) = g/\sin^2\theta$. In Fig. 7, $\bar{P}_e$ is plotted versus the S_1, for $m_d = 2.9$, $m_c = 1.5$ and several values for the correlation coefficient ρ, assuming BPSK and coherent BFSK modulation schemes. Balanced $(S_1 = S_2)$ and unbalanced $(S_2 = S_1/3)$ SIRs are also assumed here, at the two input branches.

C. Quadrature Signaling

In DQPSK with Gray coding, the conditional BER can be written as

$$\bar{P}_e(t) = \frac{1}{2\pi}\int_0^{\pi} \frac{1}{\sqrt{2}-\cos\theta} e^{-t(2-\sqrt{2}\cos\theta)} d\theta. \quad (22)$$

Again capitalizing on the similarity between (16) and (22) and changing the order between summations and integration, $\bar{P}_e$ can be extracted as

$$\bar{P}_e = \frac{1}{2\pi}\sum_{i_1,i_2,n=0}^{\infty}\left(\frac{m_d}{m_c}\right)^{-(2i_1+2m_d)} \times G_2\sqrt{S_1S_2}\Gamma(2i_1+2m_d+n) \times \int_0^{\pi}\frac{1}{\sqrt{2}-\cos\theta} \times \Psi\left(2i_1+2m_d+n, 1-i_2-m_c; \frac{g(\theta)}{\frac{m_d}{m_c}\frac{1}{\sqrt{S_1S_2}}}\right) d\theta \quad (23)$$

with $g(\theta) = -(2-\sqrt{2}\cos\theta)$.

D. Multilevel Signaling

MPSK: In MPSK, the conditional BER is

$$P_e(t) = \frac{1}{\pi}\int_0^{\pi-(\pi/M)} e^{-(\sin^2(\pi/M)\log_2 M/\sin^2\theta t)} d\theta. \quad (24)$$

Working again as in Sections V-A–C, $\bar{P}_e$ in MPSK can be written as

$$\bar{P}_e = \frac{1}{\pi}\sum_{i_1,i_2,n=0}^{\infty}\left(\frac{m_d}{m_c}\right)^{-(2i_1+2m_d)} \times G_2\sqrt{S_1S_2}\Gamma(2i_1+2m_d+n) \times \int_0^{\pi-\pi/M}\Psi\left(2i_1+2m_d+n, 1-i_2-m_c; \frac{g(\theta)}{\frac{m_d}{m_c}\frac{1}{\sqrt{S_1S_2}}}\right) d\theta \quad (25)$$

with $g(\theta) = \sin^2(\pi/M)\log_2 M/\sin^2\theta$.

MDPSK: In MDPSK, the conditional BER is

$$P_e(t) = \frac{\sin\left(\frac{\pi}{M}\right)}{\pi} \times \int_0^{\pi/2}\frac{e^{-t\log_2 M[1-\cos(\pi/M)\cos\theta]}}{1-\cos\left(\frac{\pi}{M}\right)\cos\theta} d\theta. \quad (26)$$

Hence, MDPSK can be calculated as

$$\bar{P}_e = \frac{\sin\left(\frac{\pi}{M}\right)}{\pi}\sum_{i_1,i_2,n=0}^{\infty}\left(\frac{m_d}{m_c}\right)^{-(2i_1+2m_d)} G_2\sqrt{S_1S_2} \times \Gamma(2i_1+2m_d+n)\int_0^{\pi/2}\frac{1}{1-\cos\left(\frac{\pi}{M}\right)\cos\theta} \times \Psi\left(2i_1+2m_d+n, 1-i_2-m_c; \frac{g(\theta)}{\frac{m_d}{m_c}\frac{1}{\sqrt{S_1S_2}}}\right) d\theta \quad (27)$$

with $g(\theta) = \log_2 M[1-\cos(\pi/M)\cos\theta]$.

VI. Conclusion

In this paper, the performance of a dual SIR-based selection-combining system, operating over correlative Nakagami-m fading channels with arbitrary parameters, was studied. Useful analytical formulae for the pdf and cdf at the output of SC were presented. Useful analytical formulae for the SIR pdf and cdf at the outcome of SC were presented. Using these new formulae, the outage probability, the average output SIR and the average error probability for several modulation schemes were efficiently evaluated. The effects of various parameters, such as the fading severity, the input SIR unbalance, and the level of correlation to the system's performance, were also presented.

Appendix I
cdf of the SC Output SIR

The joint pdf of the instantaneous SIRs at the two input branches of SC ζ_1, ζ_2 is given by [4], [31] as

$$f_{\zeta_1,\zeta_2}(t_1,t_2) = \frac{1}{4\sqrt{t_1t_2}}\int_0^{\infty}\int_0^{\infty} f_{R_1R_2}(x_1\sqrt{t_1}, x_2\sqrt{t_2}) \times f_{r_1,r_2}(x_1,x_2)\, x_1\, x_2\, dx_1\, dx_2. \quad (28)$$

Substituting (4) and (5) in (28) and after some algebraic manipulations, $f_{\zeta_1,\zeta_2}(t_1,t_2)$ can be written as in (29), shown at the bottom of the page. Using the infinite series representation of the modified Bessel function [23, eq. (8.445)]

$$I_\nu(z) = \sum_{k=0}^{\infty}\frac{z^{\nu+2k}}{2^{\nu+2k}k!\,\Gamma(\nu+k+1)} \quad (30)$$

and changing the order of summation and integration (since the quantity in the produced double sum is Riemann integrable and

$$f_{\zeta_1,\zeta_2}(t_1,t_2) = \frac{4m_d^{m_d+1}m_c^{m_c+1}(\sqrt{t_1t_2})^{m_d-1}(\sqrt{\rho})^{-(m_d+m_c-2)}}{\Gamma(m_d)\Gamma(m_c)\sqrt{\Omega_{d1}\Omega_{d2}}^{m_d+1}\sqrt{\Omega_{c1}\Omega_{c2}}^{m_c+1}(1-\rho)^2}\int_0^{\infty}\int_0^{\infty}(x_1x_2)^{m_d+m_c+1} \times e^{-\left((m_dt_1\sqrt{\Omega_{c1}\Omega_{c2}}+m_c\sqrt{\Omega_{d1}\Omega_{d2}})x_2^1+(m_d\sqrt{\Omega_{c1}\Omega_{c2}}+m_c\sqrt{\Omega_{d1}\Omega_{d2}})x_2^2\right)\sqrt{\Omega_{c1}\Omega_{c2}}\sqrt{\Omega_{d1}\Omega_{d2}}(1-\rho)} \times I_{m_d-1}\left(\frac{2m_d\sqrt{\rho}\sqrt{t_1t_2}x_1x_2}{\sqrt{\Omega_{d1}\Omega_{d2}}(1-\rho)}\right) I_{m_c-1}\left(\frac{2m_c\sqrt{\rho}x_1x_2}{\sqrt{\Omega_{c1}\Omega_{c2}}(1-\rho)}\right) dx_1dx_2. \quad (29)$$

converges uniformly in the range $(0, \infty)$, the joint pdf of ζ_1, ζ_2 can be written, after some algebraic manipulations, as

$$\begin{aligned} f_{\zeta_1,\zeta_2}(t_1 t_2) = & \frac{4 m_d^{2m_d} m_c^{2m_c}}{\Gamma(m_d)\Gamma(m_c)(\Omega_{d1}\Omega_{d2})^{m_d}(\Omega_{c1}\Omega_{c2})^{m_c}} \\ & \times \frac{(t_1 t_2)^{m_d-1}}{(1-\rho)^{m_d+m_c}} \\ & \times \sum_{i_1,i_2=0}^{\infty} \frac{m_d^{2i_1} m_c^{2i_2} \rho^{i_1+i_2}}{i_1! i_2! \Gamma(m_d+i_1)\Gamma(m_c+i_2)} \\ & \times \frac{(t_1 t_2)^{i_1} C_1 C_2}{(\Omega_{d1}\Omega_{d2})^{i_1}(\Omega_{c1}\Omega_{c2})^{i_2}(1-\rho)^{2(i_1+i_2)}} \end{aligned} \tag{31}$$

where C_1 and C_2 are shown at the bottom of the page. The integrals C_1 and C_2 can be solved as [23, eq. (3.326/2)]

$$\begin{aligned} C_1 = & \frac{\Gamma(i_1+i_2+m_d+m_c)}{2\left[\frac{m_d\sqrt{\Omega_{c1}\Omega_{c2}}\zeta_1 + m_c\sqrt{\Omega_{d1}\Omega_{d2}}}{\sqrt{\Omega_{d1}\Omega_{d2}}\sqrt{\Omega_{c1}\Omega_{c2}}(1-\rho)}\right]^{i_1+i_2+m_d+m_c}} \\ C_2 = & \frac{\Gamma(i_1+i_2+m_d+m_c)}{2\left[\frac{m_d\sqrt{\Omega_{c1}\Omega_{c2}}\zeta_2 + m_c\sqrt{\Omega_{d1}\Omega_{d2}}}{\sqrt{\Omega_{d1}\Omega_{d2}}\sqrt{\Omega_{c1}\Omega_{c2}}(1-\rho)}\right]^{i_1+i_2+m_d+m_c}} \end{aligned} \tag{32}$$

and (31) can finally be written as

$$\begin{aligned} f_{\zeta_1,\zeta_2}(t_1, t_2) = & \sum_{i_1,i_2=0}^{\infty} \frac{D_1 D_2 (t_1 t_2)^{i_1+m_d-1}}{(S_1 S_2)^{m_d+i_1}} \\ & \times \frac{1}{\left[\left(\frac{m_d}{m_c}\frac{t_1}{\sqrt{S_1 S_2}}+1\right)\left(\frac{m_d}{m_c}\frac{t_2}{\sqrt{S_1 S_2}}+1\right)\right]^{i_1+i_2+m_d+m_c}} \end{aligned} \tag{33}$$

where

$$D_1 = \frac{(1-\rho)^{m_d+m_c}}{\Gamma(m_d)\Gamma(m_c)}\left(\frac{m_d}{m_c}\right)^{2m_d+2i_1}$$

and

$$D_2 = \frac{\rho^{i_1+i_2}(\Gamma(i_1+i_2+m_d+m_c))^2}{i_1! i_2! \Gamma(m_d+i_1)\Gamma(m_c+i_2)}.$$

The bivariate (joint) cdf of ζ_1, ζ_2 is derived as

$$F_{\zeta_1,\zeta_2}(t_1, t_2) = \int_0^{t_1}\int_0^{t_2} f_{\zeta_1,\zeta_2}(x_1, x_2)\, dx_1 dx_2 \tag{34}$$

and using (33)

$$\begin{aligned} F_{\zeta_1,\zeta_2}(t_1, t_2) = & \sum_{i_1,i_2=0}^{\infty} \frac{D_1 D_2}{(S_1 S_2)^{m_d+i_1}} \\ & \times \int_0^{t_1} \frac{\zeta_1^{i_1+m_d-1}}{\left(\frac{m_d}{m_c}\frac{x_1}{\sqrt{S_1 S_2}}+1\right)^{i_1+i_2+m_d+m_c}} d\zeta_1 \\ & \times \int_0^{t_2} \frac{\zeta_2^{i_1+m_d-1}}{\left(\frac{m_d}{m_c}\frac{x_2}{\sqrt{S_1 S_2}}+1\right)^{i_1+i_2+m_d+m_c}} d\zeta_2. \end{aligned} \tag{35}$$

The cdf of the dual SIR-based SC output could be derived from (35), equating the two arguments $t_1 = t_2 = t$ and using [23, (3.194/1)] as

$$\begin{aligned} F_{\zeta}(t) = & \sum_{i_1,i_2=0}^{\infty} \frac{D_1 D_2}{\left(\frac{1}{t}\right)^{2m_d+2i_1}(i_1+m_d)^2 (S_1 S_2)^{m_d+i_1}} \\ & \times \left[{}_2F_1\left(i_1+i_2+m_d+m_c, i_1+m_d; i_1+m_d \right.\right. \\ & \left.\left. +1; -\frac{m_d\, t}{m_c\sqrt{S_1 S_2}}\right)\right]^2. \end{aligned} \tag{36}$$

From [23, (9.131/1)] and after some manipulations, (7) is derived.

Appendix II
pdf of the SC Output SIR

The pdf at the output of the SC can be found as

$$\begin{aligned} f_{\zeta}(t) = & \frac{d}{dt} F_{\zeta}(t) \\ = & \sum_{i_1,i_2=0}^{\infty} \frac{2 D_1 D_2}{(S_1 S_2)^{m_d+i_1}} \\ & \times \frac{t^{i_1+m_d-1}}{\left(\frac{m_d}{m_c}\frac{t}{\sqrt{S_1 S_2}}+1\right)^{i_1+i_2+m_d+m_c}} \\ & \times \int_0^{t} \frac{u^{i_1+m_d-1}}{\left(\frac{m_d}{m_c}\frac{u}{\sqrt{S_1 S_2}}+1\right)^{i_1+i_2+m_d+m_c}} du. \end{aligned} \tag{37}$$

$$\begin{aligned} C_1 = & \int_0^{\infty} x_1^{2i_1+2i_2+2m_d+2m_c-1} e^{-x_1^2\left(m_d t_1\sqrt{\Omega_{c1}\Omega_{c2_c}} + m_c\sqrt{\Omega_{d1}\Omega_{d2}}\right)/\sqrt{\Omega_{d1}\Omega_{d2}}\sqrt{\Omega_{c1}\Omega_{c2}}(1-\rho)} dx_1 \\ C_2 = & \int_0^{\infty} x_2^{2i_1+2i_2+2m_d+2m_c-1} e^{-x_2^2\left(m_d t_2\sqrt{\Omega_{c1}\Omega_{c2}} + m_c\sqrt{\Omega_{d1}}\Omega_{d2}\right)/\sqrt{\Omega_{d1}\Omega_{d2}}\sqrt{\Omega_{c1}\Omega_{c2}}(1-\rho)} dx_2. \end{aligned}$$

The integral in (37) can be solved using [23, (3.194/1)], resulting in

$$f_{\zeta}(t) = \sum_{i_1,i_2=0}^{\infty} \frac{2D_1D_2}{(S_1S_2)^{m_d+i_1}} \times \frac{t^{2i_1+2m_d-1}}{(i_1+m_d)\left(\frac{m_d}{m_c}\frac{t}{\sqrt{S_1S_2}}+1\right)^{i_1+i_2+m_d+m_c}} \times {}_2F_1\left(i_1+i_2+m_d+m_c, i_1+m_d; i_1+m_d+1; -\frac{m_d t}{m_c\sqrt{S_1S_2}}\right) \quad (38)$$

or again using [23, eq. (9.131/1)], (8) is derived.

ACKNOWLEDGMENT

The author thanks D. A. Zogas for his help in the numerical evaluation of the presented mathematical analysis, N. C. Sagias for the validation of the SC output pdf curves by simulations (Fig. 1), and S. A. Kotsopoulos for his helpful discussions. Also, he would like to thank the anonymous reviewers and the Editor, T. Lok, for their valuable comments that considerably improved the quality of this paper.

REFERENCES

[1] J. G. Proakis, *Digital Communications*. New York: McGraw-Hill, 1995.

[2] M. K. Simon and M.-S Alouini, *Digital Communication Over Fading Channels*, 1st ed. New York: Wiley, 2000.

[3] E. A. Neasmith and N. C. Beaulieu, "New results in selection diversity," *IEEE Trans. Commun.*, vol. 46, pp. 695–704, May 1998.

[4] S. Okui, "Effects of CIR selection diversity with two correlated branches in the m-fading channel," *IEEE Trans. Commun.*, vol. 48, pp. 1631–1633, Oct. 2000.

[5] S. Kozono, "Co-channel interference measurement method for mobile communications," *IEEE Trans. Veh. Technol.*, vol. 36, pp. 7–13, Jan. 1987.

[6] R. D. Yates, "A framework for uplink power control in cellular radio systems," *IEEE J. Select. Areas Commun.*, vol. 13, pp. –AU: PLEASE PROVIDE PAGE RANGE —ED., Sept. 1995.

[7] S. Yoshida, A. Hirai, G. L. Tan, H. Zhou, and T. Takeuchi, "In-service monitoring of multipath delay-sparead and C/I for QPSK signal," in *Proc. IEEE 42nd Vehicular Technolology Conf.*, Denver, CO, Apr. 1992, pp. 592–595.

[8] M. D. Austin and G. L. Stuber, "In-service signal quality estimation for TDMA cellular systems," in *Proc. PIMRC '95*, Toronto, ON, Canada, Sept. 1995, pp. 836–840.

[9] A. L. Brandao, L. B. Lopez, and D. C. McLernon, "Co-channel interference estimation for M-ary PSK modulated signals," *IEEE Wireless Pers. Commun.*, vol. 1, no. 1, pp. 23–32, 1994.

[10] C. Chayawan and V. A. Aalo, "On the outage probability of optimum combining and maximal ratio combining schemes in an interference-limited Rice fading channel," *IEEE Trans. Commun.*, vol. 50, pp. 532–535, Apr. 2002.

[11] A. Shah and A. M. Haimovich, "Performance analysis of optimum combining in wireless communications with Rayleigh fading and co-channel interference," *IEEE Trans. Commun.*, vol. 46, pp. 473–479, Apr. 1998.

[12] ——, "Performance analysis of maximal ratio combining and comparison with optimum combining for mobile radio communications with co-channel interference," *IEEE Trans. Commun.*, vol. 49, pp. 1454–1463, July 2000.

[13] V. A. Aalo and J. Zhang, "Performance analysis of maximal ratio combining in the presence of multiple equal-power co-channel interferers in a Nakagami fading channel," *IEEE Trans. Veh. Technol.*, vol. 50, pp. 497–503, Mar. 2001.

[14] ——, "On the effect of co-channel interference on average error rates in Nakagami-fading channels," *IEEE Commun. Lett.*, vol. 3, pp. 136–138, May 1999.

[15] C. M. Lo and W. H. Lam, "Performance of generalized selection combining for mobile radio communications with mixed co-channel interferers," *IEEE Trans. Veh. Technol.*, vol. 51, pp. 114–121, Jan. 2002.

[16] S. H. Tseng, "Optimum diversity combining and equalization over interference-limited cellular radio channel," *IEEE Trans. Veh. Technol.*, vol. 47, pp. 103–118, Feb. 1998.

[17] A. A. Abu-Dayya and N. C. Beaulieu, "Diversity MPSK receivers in co-channel interference," *IEEE Trans. Veh. Technol.*, vol. 48, pp. 1959–1965, Nov. 1999.

[18] J. H. Winters, "Optimum combining in digital mobile radio with co-channel interference," *IEEE J. Select. Areas Commun.*, vol. SAC-2, pp. 528–539, July 1984.

[19] A. Abu-Dayya and N. C. Beaulieu, "Outage probabilities of diversity cellular systems with co-channel interference in Nakagami fading," *IEEE Trans. Veh. Technol.*, vol. 41, pp. 343–355, Nov. 1992.

[20] M. Nakagami, "The m-distribution—A general formula if intensity distribution of rapid fading," in *Statistical Methods in Radio Wave Propagation*, W. G. Hoffman, Ed. Pergamon, U.K.: Oxford, 1960.

[21] U. Charash, "Reception through nakagami fading multipath channels with random delay," *IEEE Trans. Commun.*, vol. COM-27, pp. 657–670, Apr. 1979.

[22] T. Aulin, "Characteristics of a digital mobile radio channel," *IEEE Trans. Veh. Technol.*, vol. VT-30, pp. 45–53, Feb. 1981.

[23] I. S. Gradshteyn and I. M. Ryzhik, *Table of Integrals, Series, and Products*, 5th, Ed. New York: Academic, 1994.

[24] Y.-C. Ko, "Analysis techniques for the performance evaluation of wireless communication systems and estimation of wireless channels," Ph.D. Dissertation, University of Minnesota, Minneapolis, 2001.

[25] G. K. Karagiannidis, S. A. Kotsopoulos, and P. T. Mathiopoulos, "Generalized approach for the evaluation of the outage performance in micro- and pico-cellular networks," in *Proc. IEE—Commun.*, vol. 149, Apr. 2002, pp. 123–128.

[26] G. K. Karagiannidis and S. A. Kotsopoulos, "Outage performance considerations in mobile cellular networks," in *Quality and Reliability of Large Scale Telecommunications Systems*. New York: Wiley, 2003.

[27] M. Abramovitz and I. A. Stegun, *Handbook of Mathematical Functions with Formulas, Graphs, and Mathematical Tables*, 9th ed ed. New York: Dover, 1972.

[28] Y.-K. Ko, M.-S. Alouini, and M. K. Simon, "Average SNR of dual selection combining over correlated Nakagami-m fading channels," *IEEE Commun. Lett.*, vol. 4, pp. 12–14, Jan. 2000.

[29] M. K. Simon and M.-S. Alouini, "A unified performance analysis of digital communications with dual selective combining diversity over correlated Rayleigh and Nakagami-m fading channels," *IEEE Trans. Commun.*, vol. 47, pp. 33–43, Jan. 1999.

[30] J. W. Craig, "A new, simple, and exact result for calculating the probability of error for two-dimensional signal constellations," in *Proc. IEEE Military Communications Conf. (MILCOM'91)*, McLean, VA, Oct. 1991, pp. 571–575.

[31] C. W. Helstrom, *Probability and Stochastic Processes for Engineers*, 2nd ed ed. New York: MacMillian, 1991.

George K. Karagiannidis (M'97) was born in Pithagorion, Samos Island, Greece. He received the Diploma in 1987 and the Ph.D. degree in 1999, both in electrical engineering, from the University of Patras, Patras, Greece.

From 1990 to 1993, his research focused on the development of interfaces for diffuse IR communications links. Since 1994, he has been developing performance evaluation tools and optimum techniques for the improvement of QoS and GoS in mobile communication systems. In 2000, he joined the Institute of Space Applications and Remote Sensing, National Observatory of Athens, Athens, Greece, as a Researcher. Since 2000, he has been an Advisor for the Minister of Transports and Communications in the areas of terrestrial and satellite wireless networks. He has published and presented more than 60 technical papers in scientific journals and proceedings of conferences and is coauthor of a Greek book on mobile communications. His research interests include performance analysis of wireless communications systems, communications theory, digital communications over fading channels, interference problems, and QoS in wireless networks.

Dr. Karagiannidis is a Member of the Technical Chamber of Greece.